УДК 502.5:630*431.5:528.854

Risk assessment of adsorbed radionuclide emission by fire within Fukushima exclusion zone using multispectral satellite imagery

Sergey Stankevich [1] *, Aleksey Sakhatsky [1], Dmitry Bobro [2], Akira Iwasaki [3], Shinichi Nakasuka [3], Seiji Yoshimoto [3], Yoshihide Aoyanagi [3]

[1] *Scientific Centre for Aerospace Research of the Earth, Ukraine*

[2] *National Institute for Strategic Studies, Ukraine*

[3] *University of Tokyo, Japan*

The radionuclide emission risk assessment is very important to mitigate the impact of a nuclear accident. Based on the experience in Chernobyl, we evaluated risks in Fukushima exclusion zone for long term management using remote sensing and empirical radionuclide data. The possible emission of plant-accumulated radionuclide is incorporated into the known models for wildfire ignition and spread. Satellite data acquiring enables continuous monitoring of wildfire hazard.

Keywords: remote sensing, multispectral imagery classification, fire risk, radionuclide emission, Fukushima exclusion zone

1. Introduction

Satellite monitoring is an important and useful tool for natural resources state assessment inside the exclusion zone, as well as an effective way of the potential hazards risks mapping. One of the most dangerous hazard is the fire emergence on the areas contaminated with radionuclides. In this case, the radionuclides adsorbed by plants will be emitted up to atmosphere that would be resulted in the contamination zone expansion. Fire threat grows especially inside territories left unattended. The threat of dangerous secondary emission of radionuclides due to a wildfire in Chernobyl Exclusion Zone (ChEZ) still up to now [4]. This threat has strengthened in the summer of 2012, 2013, and 2014.

In previous work the fire risk assessment in the Chernobyl exclusion zone using satellite data (SPOT-4, 14.07.1998) was carried out on a nominal level without the use of the presented model of the risk of secondary contamination with radionuclides. The segmentation of the area concerning the fire risk (high, medium, low level) was based on the classification of satellite image with the identification of plots where the pine forests affected by pine moth. These forests are deadwood in severe and in some cases even with medium stage of impact. Besides the water index calculated according SPOT-4 also was considered for evaluation, of land cover moisture [9].

The paper is organized as follows. Section 2 describes a numerical model for fire risk assessment. Section 3 presents ecological analysis and classification of the basic types of biotopes within the study area. Section 4 discusses the preliminary results obtained by multispectral satellite imagery processing. Section 5 makes this research conclusions.

2. Risk assessment model

Main score values of fire danger in mapping of radionuclide emission risk should be considered an ignition probability P and a fire potential area A [2]. In this case the risk at the point (x, y) of a possible fire accident can be evaluated as

$$Risk(x,y) = P(x,y)\cdot Z(x,y), \qquad (1)$$

where Z(x, y) is the adsorbed radionuclide content in vegetation fuel per area unit. Accordingly, the radionuclide emission total hazard within A will be

$$Hazard\ (A) = \int_A P(x,y)\cdot Z(x,y)\,dx\,dy\ . \qquad (2)$$

Hazard prescribe in integral form (2) requires quite a sophisticated geospatial simulation taking into account terrain elevations, wind direction, natural fuel specifications, etc. Typically, many of these data are unavailable or highly dynamic. Therefore, we had to accept a significant simplification of the model. In particular, if we consider the rate of fire spread R over ground as uniformly isotropic, and spatial distribution of the radionuclide content as constant, then the (2) equation may be rewritten

$$Hazard(x,y) = \pi P(x,y)\cdot Z(x,y)\cdot [R(x,y)\cdot dt]2, \qquad (3)$$

where dt is the time period of analysis. It is obvious that dt cannot be too large.

3. Fire spread model

To evaluate the ignition probability the Schroeder's (1969) spontaneous ignition model [14] and the Latham's (1979) model of ignition by lightning [8] were used:

* e-mail: st@casre.kiev.ua

Online ISSN 2313-2132

$$P'(x,y) = \frac{0.000048\chi^{4.3}(x,y)}{50}, \quad (4)$$

where $P'(x,y)$ is the spontaneous ignition probability,

$$\chi(x,y) = \frac{400 - Q'(x,y)}{10}, \quad (5)$$

where $Q'(x,y)$ is the heat of preignition, the energy per unit mass required for ignition, which approximated as

$$Q'(x,y) \approx 138.77 + 619.57w(x,y), \quad (6)$$

where $w(x,y)$ is vegetation water content fraction.

$$P''(x,y) \approx 0.64 \exp[-0.072w(x,y)] \quad (7)$$

is the probability of ignition by lightning approximation. Aggregated probability of ignition was calculated as the joint probability of independent events:

$$P(x,y) = 1 - [1 - P'(x,y)]\cdot[1 - P''(x,y)]. \quad (8)$$

The rate of fire spread is described by Rothermel's (1972) fire spread model with minor adjustments by Albini (1976) [12]:

$$R(x,y) = \frac{I(x,y)\xi(x,y)[1+u(x,y)+s(x,y)]}{\rho(x,y)\varepsilon(x,y)Q(x,y)}, \quad (9)$$

where $I(x,y)$ is reaction intensity, the energy release rate per unit area of fire front, $\zeta(x,y)$ is a propagating flux ratio, $u(x,y)$ is a wind multiplier, $s(x,y)$ is a slope multiplier, $\rho(x,y)$ is an amount of fuel per unit volume, $\varepsilon(x,y)$ is an ignition proportion, $Q(x,y)$ is the heat of preignition. The main variables in (9) are determined by the following semi-empirical equations:

$$I(x,y) = \Gamma(x,y)\cdot m(x,y)\cdot h(x,y)\cdot[1-w(x,y)]\cdot\eta, \quad (10)$$

where $\Gamma(x,y)$ is reaction velocity, the energy release rate per unit area of fire front, $m(x,y)$ is a net fuel loading, $h(x,y)$ is the heat content of the fuel, commonly h = 19.6 .. 21.4 MJ/kg for dry vegetation and $h \approx 10$ MJ/kg for fresh one; η is a mineral damping coefficient, its normal value is $\eta = 0.3074 \ldots 0.3207$;

$$\Gamma(x,y) \approx \Gamma_{max}(x,y)\cdot\exp[8.0933\sigma(x,y)^{-0.8189}], \quad (11)$$
$$\Gamma_{max}(x,y) \approx [0.0591 + 2.926\sigma(x,y)^{-1.5}]^{-1},$$

where $\sigma(x,y)$ is a surface-area-to-volume ratio of natural fuel. With regard $\frac{m}{\rho} \equiv \delta$ *i.g.* fuel depth, the (9) equation becomes

$$R(x,y) = \frac{I(x,y)\xi(x,y)[1+u(x,y)+s(x,y)]}{\rho(x,y)\varepsilon(x,y)Q(x,y)}, \quad (12)$$

where the following approximations may be used:
$Q(x,y) \approx 581 + 2594\, w(x,y)$,

$$Q(x,y) \approx 581 + 2594\, w(x,y), \quad (13)$$

$$\varepsilon(x,y) \approx \exp\left[-\frac{4.528}{\sigma(x,y)}\right] \quad (14)$$

$$\zeta(x,y) \approx \frac{\exp[0.792+3.7597\sigma(x,y)^{0.5}]}{192+7.9095\sigma(x,y)} \quad (15)$$

$$u(x,y) \approx 0.715\exp[-0.8711\sigma(x,y)^{0.55}]\cdot(3.281v)^{0.15988?(x,y)0.54}, \quad (16)$$

$$s(x,y) \approx 5.275^{-1}\,\mathrm{tg}^2[\varphi(x,y)], \quad (17)$$

where v is the wind velocity at midflame height, $\varphi(x,y)$ is an angle of slope.

4. Radionuclide transfer model

In the first phase of radioactive contamination spreading after a nuclear accident, directly deposited to vegetation cover radionuclides produce the main contribution to the fire risk [3]. In this case, the quantity of radionuclides emitted by fire is simply proportional to contamination level of the territory:

$$Z(x,y) = \zeta Z_0(x,y), \quad (10)$$

where $Z_0(x,y)$ is a total surface contamination by radionuclides, ζ is a fraction of radionuclides, deposited in vegetation fuel. This value is typically less than 0.1–0.15.

After 1–2 years after a nuclear accident, the main source of radioactive emission in case of fire are radionuclides adsorbed by annuals and perennials from the contaminated soil.

Values of soil to plant radionuclides transfer factors (TF) are significantly different for various soil types [1]. The TF for ^{137}Cs are 7–15 times higher for all vegetation types on the peat-swampy soils than on the soddy-podzolic, 10–20 times higher than on the grey forest, and 15–30 times higher than on the chernozem ones. The TF values for ^{90}Sr are 5 times lower on the grey forest soils and 10 times lower on the chernozems than on the soddy-podzolic soils [7].

One can notice that it is almost impossible to determine experimentally the TF in the year of radionuclides fallouts because plants contamination after the accident is mainly stipulated by the surface radionuclides precipitation. The simulated TF values for the moment of radionuclides fallouts for the ChEZ are given in Table 1 [11, 13].

In addition it is determined that the TF values are decreased at time. And the main factor changing the radiation condition on the contaminated territories is considered to be the radionuclides immobilization with a soil absorbing complex. The velocity of the radionuclides accumulation factors (AF) decrease at the expense of this process for ^{137}Cs and ^{90}Sr is significantly

Table 1
The TF values for ^{137}Cs, $kg^{-1} \cdot m^2$

Vegetation type	Peat-swampy soil	Soddy-podzolic soil	Grey forest soil
natural grass	223	29	10
coniferous forest	0.02	0.0017	0.0005
broad-leaved forest	0.02	0.002	0.0007

higher, than because of natural decay. So, for the period after the Chernobyl accident, the TF values for radionuclides transfer into plans have decreased for ^{137}Cs by approximately 100 times on the organic soils, by 10–30 times — on the mineral ones; and for ^{90}Sr — by 2–3 times on the mineral soils. At the same time, it is forecasted a significant further slowing-down of auto-rehabilitation processes; and a decrease of plants contamination is supposed to be determined by half-decay periods of ^{137}Cs and ^{90}Sr (Fig. 1).

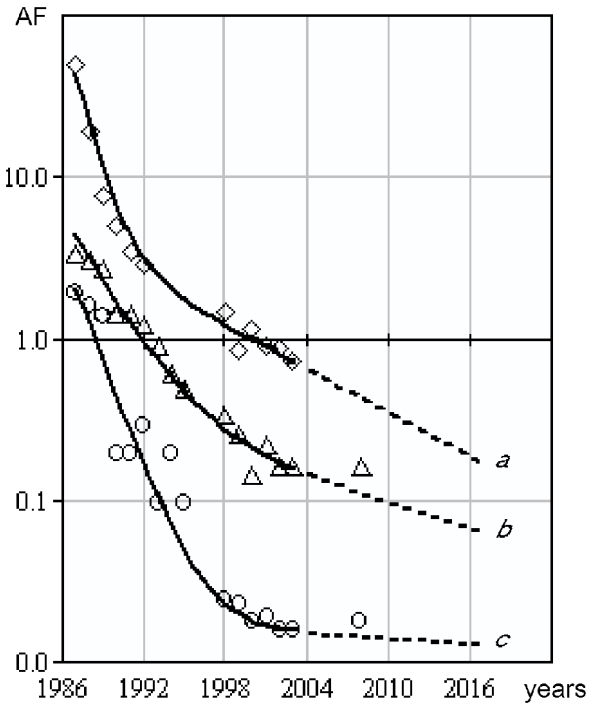

Figure 1. The TF dynamics for ^{137}Cs of natural grass on the peat-swampy soils (a), soddy-podzolic soils (b) and chernozems (c)

As to the forest ecosystems, the character of their radiation contamination is essentially different because of their complicated vertical structure and significant volume of over-ground phytomass. Right after the radionuclides precipitation, their vertical migration starts from the upper phytocenosis layers to the soil surface.

Long-term research of ^{90}Sr and ^{137}Cs distribution in the pine forest biocenosis of the ChEZ shows that the main part of ^{90}Sr and ^{137}Cs (76–83%) is located in the soil, 6-13% is accumulated with the forest bedding, 6–10% is kept in the leaf canopy, and the mossy cover contains the rest (1–5%). The trees' steams are considered to be a main depot for the balk content of radionuclides (36–53%) in the over-ground part of forest plants [16].

It is determined that with time, the increase of a specific activity of ^{137}Cs in the majority components of timber stands — sprouts, leaves, bark, wood — occurs in almost all wood species (Fig. 2) [5].

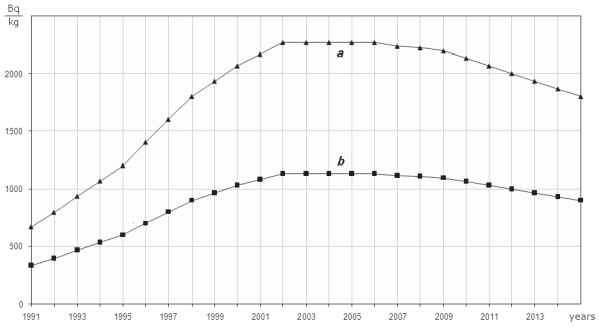

Figure 2 . Long-term dynamics of a specific activity of ^{137}Cs in Scotch pine wood when density of radiation contamination of soil equaled ^{370} kBq/m^2 (a) and ^{185} kBq/m^2 (b)

5. Study area

Fukushima exclusion zone includes the following types of landscapes: urban/suburban area, abandoned farmlands, coastal area and highland forests.

The study area is clearly divided into plain coastal zone and mountain area. The coastal zone is about 7 km wide in the region of the Fukushima NPP. It is a plain with low hills dissected by shallow and broad valleys of small rivers and streams. Further inland from the coast, the mountainous part begins, where the absolute level of relief achieved approximately 60–90 meters. In the mountainous part the relief reaches of about 1 km above sea level over a distance of about 30 km from the coast. The mountainous part is sufficiently dissected by deep valleys of numerous small rivers and streams. The depth of the valleys is up to several hundred meters (200–300 m).

The mountainous part of the territory and the hills of the plain area are covered by forests. Those are mainly mixed coniferous and broad leaves ever green and deciduous forests. There are areas of homogeneous pine and cedar forests of different ages.

For pre-classification the territory within Fukushima-1 area has been selected. It is about 20 × 20 km. The classification was carried out on the base of Landsat-5/TM image (http://earthexplorer.usgs.gov) on April 5,

2011 (Fig.1a). During the pre-classification, carried out by different methods, the following classes of land cover have been classified: 1) the mainly coniferous forests; 2) the predominantly broad leaves forests; 3) the mixed forests, 4) the grassy vegetation of meadows on watersheds, river valleys and within abandoned farmlands; 5) the man-made objects, 6) settlements 7) wet areas of river valleys and abandoned rice paddies; 8) the surface of water bodies (lakes, rivers, ponds).

The classification results by different methods were similar. According to the method of maximum likelihood (ML) and minimum distance (MD) supervised classification (Fig.1d) the following relation of classes within the land are observed (Table 2).

Table 2
Statistics of land cover classification of study area

Class of land cover	%
red pine forests	26.70
cedar forests	4.86
cypress forests	2.39
black pine forests	0.69
other broad-leaved forests	35.48
larch forests	3.51
oak forests	1.77
meadows	6.53
wetlands	2.17
settlements	4.36
barren lands and man-made surfaces	1.24
water bodies	10.30
Total	100.0

Mixed forests occupy the largest area, more than 35%, coniferous forests cover the area more than 23%, deciduous forest is about 20%. A large area is occupied also by grassy vegetation of watersheds and river valleys within the meadows and the farmlands (about 15%). Field-survey within Fukushima exclusion zone revealed that there are many abandoned dried rice fields. Other classes take considerably less area.

6. Results and discussion

The developed risk assessment model was applied to test site within Fukushima exclusion zone using Landsat-5/TM multispectral satellite imagery (April 5, 2011, Fig.3a), ASTER GDEM digital terrain elevations data (DTED, http://gdem.ersdac.jspacesystems.or.jp), October 17, 2011, (Fig.3c) and results of airborne monitoring of cesium surface deposition by the Ministry of Education, Culture, Sports, Science and Technology (MEXT) of Japan (http://www.mext.go.jp/english/incident/1303962.htm), May 6, 2011, (Fig.3e). All seven spectral bands of TM sensor have been precalibrated and converted into the land surface spectral reflectance to avoid the influence of solar irradiance and atmosphere. The water content fraction (Fig.3b) was calculated using the normalized water index (NWI) with the shortwave infrared (SWIR) TM band [10].

The maximum likelihood (ML) and minimum distance (MD) supervised classification were carried out using ground-based truth area of interest (AOI) for each class/subclass. The outputs are shown in Fig.3d.

Theoretical models of wildfire accident and spread were adapted and debugged using U.S. Forest Service BehavePlus fire behavior simulation system [6]. The values of model parameters to perform computations over the study area were collected from the specifications of the most suitable biotopes, documented by the U.S. Forest Service [15].

As a result the maps of spatial distribution of the point source fire ignition probability (8) and integral hazard of adsorbed radionuclide emission by fire (3) were obtained within the study area. These maps are shown in Fig.3f and Fig.3g, respectively.

The greatest risk of radionuclide emission by wildfire within the exclusion zone occurs in the central and north-western parts, mainly inside the cypress and red pine forest biotopes. Integral risk over land cover classes of study area is distributed as shown in Table 3.

Table 3
Average risk of radionuclide emission by wildfire over land cover classes

Class of land cover	Average risk (Ci/min)
red pine forests	23.4
cedar forests	20.3
cypress forests	36.2
black pine forests	14.1
other broad-leaved forests	0.97
larch forests	2.64
oak forests	1.91
meadows	0.51
wetlands	–
settlements	–
barren lands and man-made surfaces	–
water bodies	–
Average over land area	10

Coniferous forests in the foothills within the Fukushima disaster area are under greatest hazard of radionuclide secondary emission. Depending on weather conditions and season the spatial distribution of hazard can be varied significantly.

7. Conclusions

So, we have developed a complete geoinformation technology for quantitative assessment and mapping the risk of radionuclide secondary emission as a result of wildfire inside radioactive contaminated area. Described technology takes into account both the spontaneous ignition probability / fire spread rate and the density of radioactive contamination of ground. Known models of wildfire environment were used, which are based on the natural fuel water content, terrain elevations data, wind conditions and soil-to-vegetation radionuclide transfer. A significant sea-

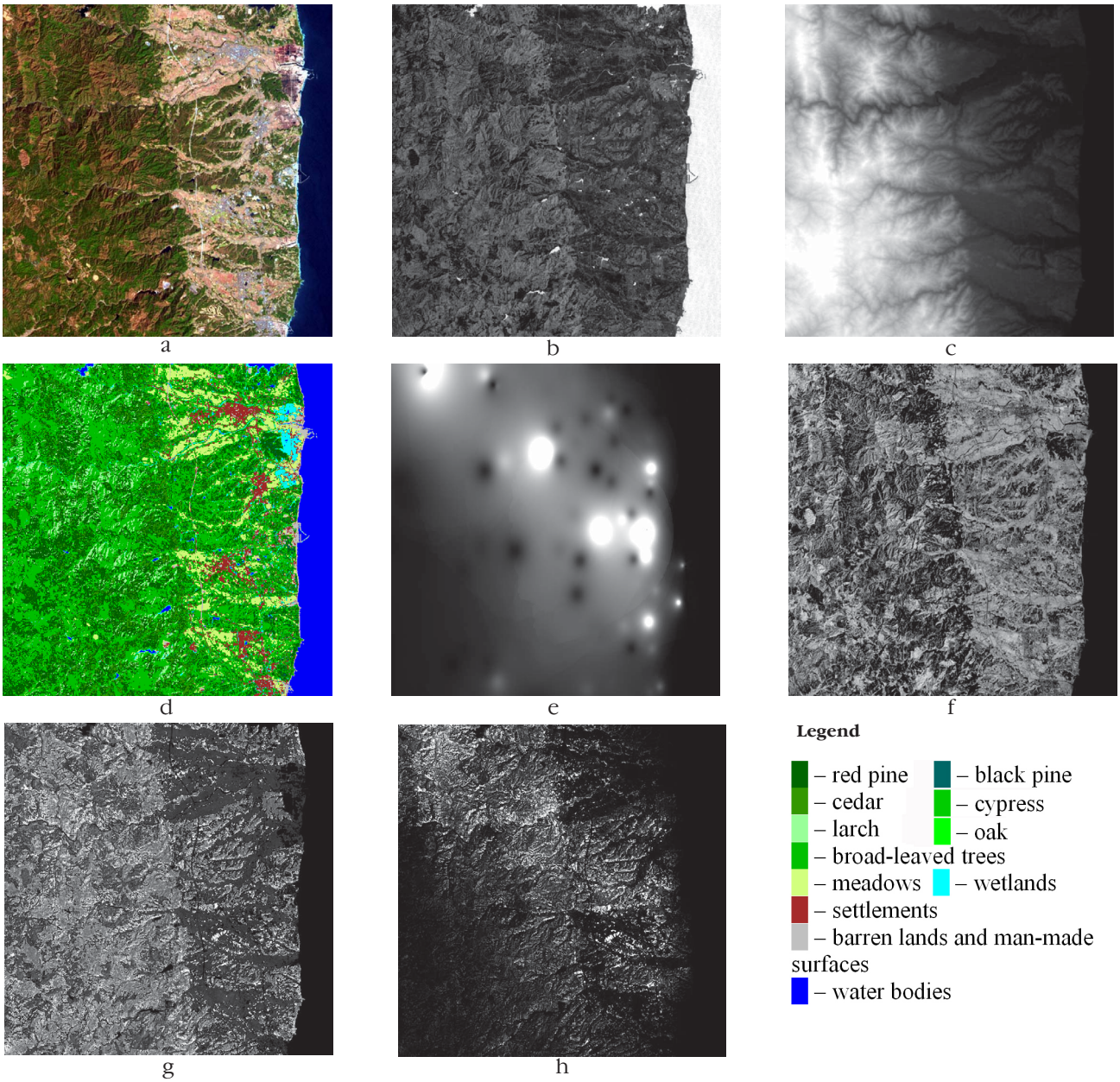

Figure 3. Risk mapping of adsorbed radionuclide emission by fire over Landsat-5/TM multispectral satellite imagery of Fukushima disaster zone
a – color-composite Landsat-5/TM image, b – normalized water fraction, c – terrain elevations (m), d – ML/MD classification result, e – map of vegetation adsorbed radionuclide content (Bq/m^2), f – ignition probability distribution map, g – rate of fire spread (m/min) distribution map, h – final map of radionuclide emission total hazard (Ci/min)

sonal variability of wildfire hazard requires continuous operational satellite-based monitoring of radioactive contaminated area.

The continuous joint research is needed towards the improvement of risk assessment models for Fukushima and Chernobyl exclusive areas.

Acknowledgements

This research was commissioned by the University of Tokyo (2013-2015) with the financial support of Ministry of Education, Culture, Sports, Science and Technology of Japan according to government agreement. We would like to pay our compliments to Ministry of Foreign Affairs of Japan for contributing our research.

References

1. Absalom J. P. Predicting soil to plant transfer of radiocaesium using soil characteristics / J. P. Absalom, S. D. Young, N. M. J. Crout, A. F. Nisbet, R. F. M. Woodman, E. Smolders, A.G. Gillett // Environmental Science & Technology.— 1999. — Vol.33. — No. 8. — P. 1218–1223.
2. Bedford T. J. Probabilistic Risk Analysis: Foundations and Methods / T. J. Bedford, R. M. Cooke.— N. Y.: Cambridge University Press, 2001. — 414 p.
3. Dusha-Gudym S. I. Transport of radioactive materials by

wildland fires in the Chernobyl accident zone: How to address the problem / S. I. Dusha-Gudym // International Forest Fire News. — 2005. — No.32. — P. 119–125.
4. Evangeliou N. Wildfires in Chernobyl-contaminated forests and risks to the population and the environment: A new nuclear disaster about to happen? / N. Evangeliou, Y. Balkanski, A. Cozic, W.-M. Hao, A. P. Møller // Environment International. — 2014. – Vol.73.— No.12. — P. 346–358.
5. Fuhrmann M. Uptake of Cs-137 and Sr-90 from contaminated soil by three plant species: Application to phytoremediation / M. Fuhrmann, M. M. Lasat, S. D. Ebbs, L. V. Kochian, J. Cornish // Journal of Environmental Quality. — 2002. — Vol. 31. — No. 3. — P. 904–909.
6. Heinsch F. A. BehavePlus fire modeling system, version 5.0 / F. A. Heinsch, P. L. Andrews / General Technical Report RMRS-GTR-249. — Fort Collins: U. S. Forest Service, 2010. — 120 p.
7. Konoplev A.V. Parameterization of 137Cs soil-plant transfer through key soil characteristics (in Russian) / A. V. Konoplev, I. V. Konopleva // Radiation Biology. Radioecology. — 1999. — Vol. 39. — No. 4. — P. 455–461.
8. Latham D.J . Ignition probabilities of wildland fuels based on simulated lightning discharges / D. J. Latham, J. A. Schlieter / Research Paper INT-411. — Ogden: U. S. Forest Service, 1989. — 20 p.
9. Lyalko V. I., Sakhatskyi O. I. Mapping areas of high natural fire risk (in Ukrainian) // Space for Ukraine: Atlas of interpreted images of the territory of Ukraine from "Ocean-O" Ukrainian-Russian satellite and other satellites / Ed. V. I. Lyalko and O. D. Fedorovsky. — Kiev: National Academy of Sciences of Ukraine, National Space Agency of Ukraine, 2001. — P. 29–30.
10. Popov M. O. Possibilities of land cover moisture evaluation using remote sensing multispectral data for Ukrainian West Polesie / M. O. Popov, O. I. Sakhatsky, S. A. Stankevich // Nature and landscape monitoring system in the West Polesie region / Ed. by T. J. Chmielewski and C. Sławinski.— Lublin: University of life sciences, 2009. — P. 65–76.
11. Prister B. S. Experimental substantiation and parameterization of the model describing ^{137}Cs and ^{90}Sr behavior in a soil-plant system / B. S. Prister, V. G. Baryakhtar, L. V. Perepelyatnikova, V.D. Vinogradskaya, N. R. Grytsuk, T. N. Ivanova // Environmental Science and Pollution Research. — 2003.— Vol. 10.— No.1. — P. 126–136.
12. Pyne S. J. Introduction to Wildland Fire / S. J. Pyne, P. L. Andrews, R. D. Laven.– N. Y.: John Wiley, 1996. — 188 p.
13. Quantification of Radionuclide Transfers in Terrestrial and Freshwater Environments for Radiological Assessments / IAEA-TECDOC-1616 Technical Report. — Vienna: IAEA, 2009. — 622 p.
14. Schroeder M. J. Ignition probability / M. J. Schroeder / Office Report 2106-1. — Silver Spring: Environmental Science Services Administration, 1969. — 28 p.
15. Scott J. H. Standard fire behavior fuel models: a comprehensive set for use with Rothermel's surface fire spread model / J. H. Scott, R. E. Burgan / General Technical Report RMRS-GTR-153. — Fort Collins: U.S. Forest Service, 2005. — 80 p.
16. Yoschenko V. I., Kashparov V. A., Levchuk S. E., Glukhovskiy A. S., Khomutinin Y. V., Protsak V. P., Lundin S. M., Tschiersch J. Resuspension and redistribution of radionuclides during grassland and forest fires in the Chernobyl exclusion zone: Modeling the transport process // Journal of Environmental Radioactivity. — 2006. — Vol. 87. — No. 3. — P. 260–278.

ОЦІНКА РИЗИКУ ВИКИДУ АДСОРБОВАНИХ РАДІОНУКЛІДІВ ВНАСЛІДОК ПОЖЕЖІ В ЗОНІ ВІДЧУЖЕННЯ ФУКУСІМИ З ВИКОРИСТАННЯМ БАГАТОСПЕКТРАЛЬНИХ СУПУТНИКОВИХ ЗОБРАЖЕНЬ

Сергій Станкевич, Олексій Сахацький, Дмитро Бобро, Акіра Івасакі, Шінічі Накасука, Сейі Йошімото, Йошіхіде Аоянагі

Оцінка ризику емісії радіонуклідів дуже важлива для пом'якшення наслідків ядерної аваріаї. Грунтуючись на досвіді Чорнобиля, нами отримано довготривалі оцінки ризику в зоні відчуження Фукусіми з використанням дистанційного зондування і даних про зараження території радіонуклідами. Можливу емісію адсорбованих рослинами радіонуклідів поєднано з відомими моделями виникнення і поширення лісової пожежі. Залучення супутникових даних дозволяє забезпечувати безперервний моніторинг пожежонебезпеки.

Ключові слова: дистанційне зондування, класифікація багатоспектральних зображень, пожежонебезпечність, емісія радіонуклідів, зона відчуження Фукусіми

ОЦЕНКА РИСКА ВЫБРОСА АДСОРБИРОВАННЫХ РАДИОНУКЛИДОВ ВСЛЕДСТВИЕ ПОЖАРА В ЗОНЕ ОТЧУЖДЕНИЯ ФУКУСИМЫ С ИСПОЛЬЗОВАНИЕМ МНОГОСПЕКТРАЛЬНЫХ СПУТНИКОВЫХ ИЗОБРАЖЕНИЙ

Сергей Станкевич, Алексей Сахацкий, Дмитрий Бобро, Акира Ивасаки, Шиничи Накасука, Сейи Йошимото, Йошихиде Аоянаги

Оценка риска выброса адсорбированных радионуклидов очень важна для смягчения последствий ядерной аварии. Основываясь на опыте Чернобыля, мы получили долговременные оценки риска в зоне отчуждения Фукусимы с использованием дистанционного зондирования и данных о заражении территории радионуклидами. Возможная эмиссия адсорбированных растениями радионуклидов объединена с известными моделями возникновения и распространения лесного пожара. Привлечение спутниковых данных позволяет обеспечивать непрерывный мониторинг пожароопасности.

Ключевые слова: дистанционное зондирование, классификация многоспектральных изображений, пожароопасность, эмиссия радионуклидов, зона отчуждения Фукусимы